

MORPHOLOGICAL MODELLING OF STRONGLY CURVED ISLANDS

Dano Roelvink^{1,2,3}, Kees den Heijer^{2,3} and Jaap van Thiel de Vries^{2,3}

Abstract

Land reclamations and island coasts often involve strongly curved shorelines, which are challenging to be properly modeled by numerical morphological models. Evaluation of the long term development of these types of coasts as well as their response to storm conditions requires proper representation of the governing physical processes. Not all types of numerical models are equipped to represent an entire island and allow waves from any direction. In this paper we demonstrate XBeach's capabilities of plying a curvilinear grid around a small-scale circular island and exchanging model variables between the lateral boundaries by the recently implemented cyclic boundaries. The small-scale physical model tests by Kamphuis and Nairn (1984) were modeled with XBeach using both the stationary and the nonhydrostatic wave model on a rectangular as well as a curvilinear grid. The wing-bars that typically develop in Kamphuis' tests are represented in the model, albeit that the angle of the bars is different. In a different XBeach model series, we investigate the behaviour of a larger scale curved coastline model under extreme storm conditions, for varying coastal radius. The results show that maximum erosion occurs at the locations where the incident wave direction is under an angle of 45 degrees with the coastline, and the coastal radius is of secondary importance.

Key words: island, morphology, modeling, longshore transport, curved coasts, XBeach

1. Introduction

Climate-related and autonomous changes in sea levels and wave conditions motivate an urgency to understand the response of low-lying islands to these changes in order to assess impacts and mitigating measures. This paper particularly focusses on strongly curved coasts of small islands, which provide a number of challenges to morphological modellers.

In a physical sense, curved island coasts are subject to strong gradients in wave conditions and sediment transport. They usually have areas where the angle of wave incidence is larger than 45 degrees, thus potentially leading to coastline instabilities such as sand waves or spits. This may however be suppressed when the waves come from different directions. For smaller islands, the curvature is such that due to wave refraction and current advection, both delaying the longshore current, the maximum longshore current does not have to be anywhere near the location where the coast makes an angle of 45 degrees relative to the incident wave direction. As a result the longshore transport estimates based on a uniform coastline will be wide off the mark. Infragravity waves generated primarily on the upwind side of the island may propagate around the island as edge waves, gradually damping out and interacting with edge waves coming from the other side. Edge waves cause periodic oscillations in the mean water level which will change the impact of waves on the coastline and thus sediment transports.

In terms of numerical modelling, by far not all types of models are equipped to be applied around an entire island and then to allow waves to enter from any direction. Rectangular grids need excessive refinement to

¹UNESCO-IHE, P.O. box 3015, 2601 DA Delft, the Netherlands, d.roelvink@unesco-ihe.org

² Delft University of Technology, Faculty of Civil Engineering and Geosciences, Section Hydraulic Engineering, P.O. Box 5048, 2600 GA, Delft, The Netherlands

³ Deltares, Department ZKS and HYE, P.O. Box 177, 2600 MH, Delft, The Netherlands

have enough resolution everywhere. Unstructured-grid models could be applied but hitherto lack functionality to model infragravity waves. Models with a curvilinear grid such as Delft3D or XBeach (Roelvink et al., 2009) can be plied around an island, but would need cyclic boundaries to make the model continuous around the island. With an implicit scheme such as Delft3D this poses problems; however, XBeach has an explicit scheme where implementing cyclic boundaries is more straightforward.

Another issue is that for very small-scale islands such as the temporary sandy islands built to support exploration drilling in the Arctic, discussed in Kamphuis (1984), it becomes questionable whether a wave-averaged or even just short-wave averaged approach is still justified. In order to investigate this, a recently implemented functionality in XBeach, viz. a one-layer nonhydrostatic model following the formulations by Stelling and Zijlema (2003), Zijlema and Stelling (2005, 2008) and implemented by Smit (Smit et al., 2013) was tested in a first application including full morphodynamic response.

In this paper, we present simulations with the 2DH Xbeach model exploring the morphological evolution of small islands and curved coastlines. Our aim is to assess in more detail the key physical processes and parameters that shape the morphological evolution of small islands and strongly curved coastlines. In order to do this we have assessed different grids (rectangular and circular), different model approaches (stationary, surfbeat and intrawave) and the model its sensitivity to different parameters (bedroughness, grain diameter, horizontal viscosity) and input (wave height). To simulate the physical processes around circular islands a new type of boundary condition was implemented (Section 2). Subsequently in Section 3 the effect of different model approaches to simulate the morphological evolution of small circular islands is assessed. Very small-scale islands are considered where all processes are extremely non-uniform and the island undergoes significant deformation and displacement of the centre of gravity. Next in section 4, the morphological evolution of curved coastlines with larger radii are studied, in order to obtain insight in the transition to quasi-longshore uniform to strongly non-uniform behaviour.

2. Model implementation

Cyclic lateral boundaries have been implemented in XBeach in order to allow modelling of the physical phenomena around small islands as mentioned in the introduction. The basis for the implementation is the curvilinear version presented by Roelvink et al. (2012), which is presently standard functionality in the code. Cross-wise communication at the lateral boundaries between the primary variables was carefully implemented in the wave, flow, suspended transport and bed updating modules, with special attention to avalanching processes. One overlapping grid cell is enough to obtain a seamless coupling, allowing for instance infragravity waves and edge waves to cross the coupling boundary in both directions.

3. Deformation of a small temporary island

In the first example, the deformation of a temporary sandy island is studied. This case is representative of very small-scale islands where all processes are extremely non-uniform and the island undergoes significant deformation and displacement of the centre of gravity. This example is taken after small-scale physical model test by Kamphuis (1984). The island was circular and the upscaled-scale real world cross-section is shown in Figure 1.

Two grids were created to study this problem: a circular grid with approx. 3 m resolution in cross-shore and cyclic lateral boundaries, and a rectangular grid with 5 m by 5 m grid cells. Since Kamphuis' tests were carried out with regular waves the model was run in stationary mode with constant wave energy boundary conditions. All simulations were carried out at prototype scale with the upscaled storm conditions that Kamphuis used in his test. The wave conditions were unidirectional, regular with a wave height of 3 m and

a wave period of 8 s. The simulation period was 10 hours, enough to see the main developments occur.

The morphological evolution during the physical model tests was characterized by the formation of so-called 'wing bars', see Figure 2. Given the many uncertainties related to small-scale movable-bed models we have not strived for an exact reproduction but instead have investigated the mechanisms that can explain the observed morphological feature.

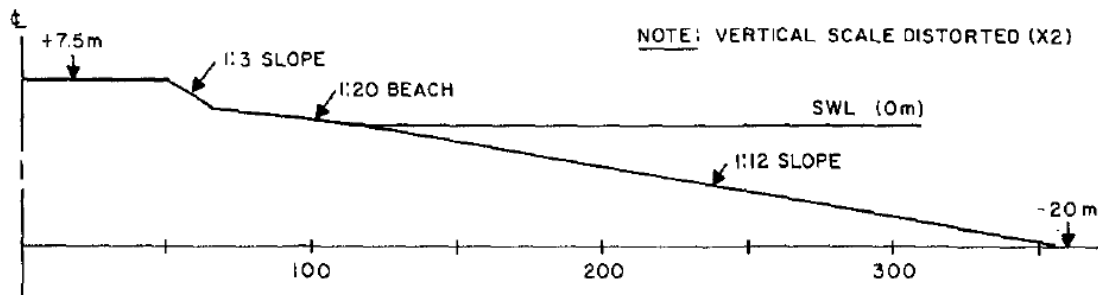


Figure 1 Cross-section of circular island test by Kamphuis (1984)

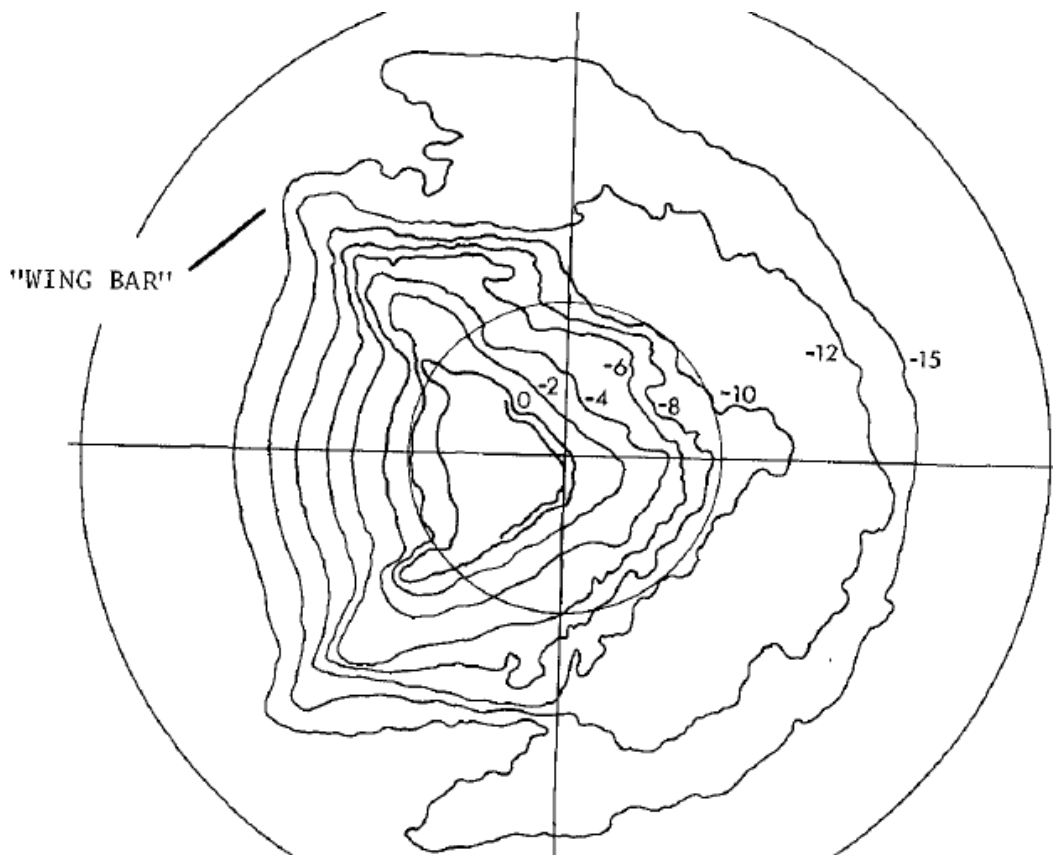


Figure 2 Deformation pattern of island in Kamphuis (1984) test.

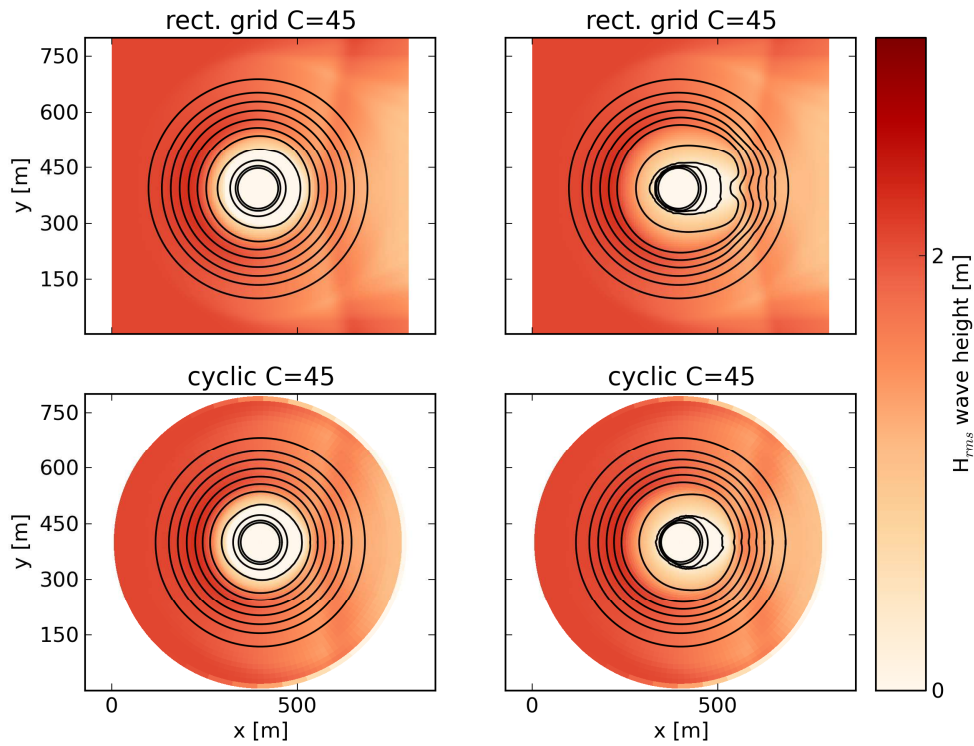


Figure 3 Wave height pattern at beginning (left panels) and end (right panels) of simulation; stationary runs, square uniform grid (top) vs. circular cyclic grid (bottom).

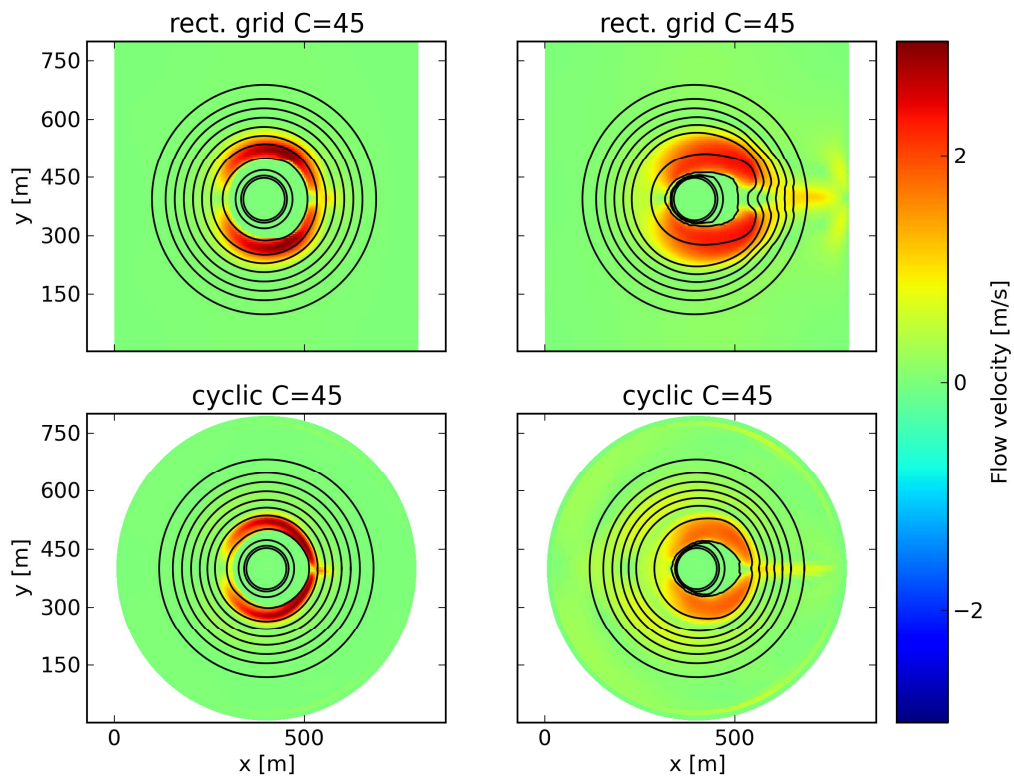


Figure 4 Pattern of mean current magnitude on initial (left panels) and final (right panels) bathymetry and depth contours, on rectangular grid with 5 m resolution (top) and circular, cyclic grid (bottom)

In Erreur ! Source du renvoi introuvable. the wave height pattern and bed contours are compared for the square grid and the circular grid, in the initial situation and after approximately 10 hours of wave action. The wave height patterns agree quite well, showing strong refraction effects with an interesting pattern of wave height behind the island which is produced in both simulations. The resulting morphological evolution however does not really tend towards the wing bars as observed in the physical model tests. In the simulation with rectangular grid there are two separate wings behind the island, though much more in downstream direction and in the model with the circular grid the longshore current wraps around the island more and deposits the sediment mostly behind the island. In both cases the most severe erosion takes place not at the upstream end of the island, but at the location where the initial coastline makes an angle of approx. 45 degrees with the incoming waves.

The current velocity patterns for both runs are compared in Figure 4. We see qualitatively comparable patterns and evolution but the circular grid leads to a sharper and more concentrated flow pattern which extends further behind the island. In the end this results in rather different morphology behind the island, though the front end is quite similar between the runs. The likely reason for the differences between the rectangular grid and circular grid is the numerical diffusion that may take place as a result of the staircase-like description of the coastline in the rectangular grid case.

We have assessed the reproduction and evolution of the wing bar pattern in both grids by varying bed roughness, wave height, grain diameter, horizontal viscosity and back boundary conditions but could find only minor qualitative changes: All simulations produced wing bars, if any, that were too much in downstream direction. Qualitatively, increased bed roughness led to some more upstream development of the wing bars; increased wave height led to even more downstream evolution; grain diameter had little effect; increasing horizontal viscosity mainly led to smoothing and having an open back boundary increased the longshore velocities somewhat.

A possible reason that the wing bars are pushed to far in downstream direction is the lack of diffraction in the wave-averaged model. As a result there is likely too much refraction around the island and hence the current patterns wrap around the island too far. To investigate this in more detail we carried out some exploratory simulations with the nonhydrostatic short-wave model implemented in XBeach. We generated sine-wave boundary conditions for the same rectangular-grid schematization of the island, to which we added a 1:10 beach to dissipate the waves, as in the physical model tests. In Figure 5 and Figure 6 we show snapshots of the current velocity pattern on the initial and final bathymetry, respectively, for different bed roughnesses characterized by Chezy values of 30, 45 and 80. Results are compared with the current velocity pattern obtained from the stationary, wave-averaged model, discussed before. We now clearly see much smaller velocities behind the islands, a clear influence of the bed roughness on the flow pattern and consequently a tendency towards wing bars development that start to approach those observed in the tests.

To clarify the difference in wave-driven current between the nonhydrostatic and stationary tests we compare the time-averaged wave height and current velocity patterns for Chezy value of 45 in Figure 7. For the wave height pattern, the nonhydrostatic model shows an interesting interference pattern between the waves refracting around either side of the island. The current patterns are similar in strength but in the nonhydrostatic case the current strength reduces much more behind the island.

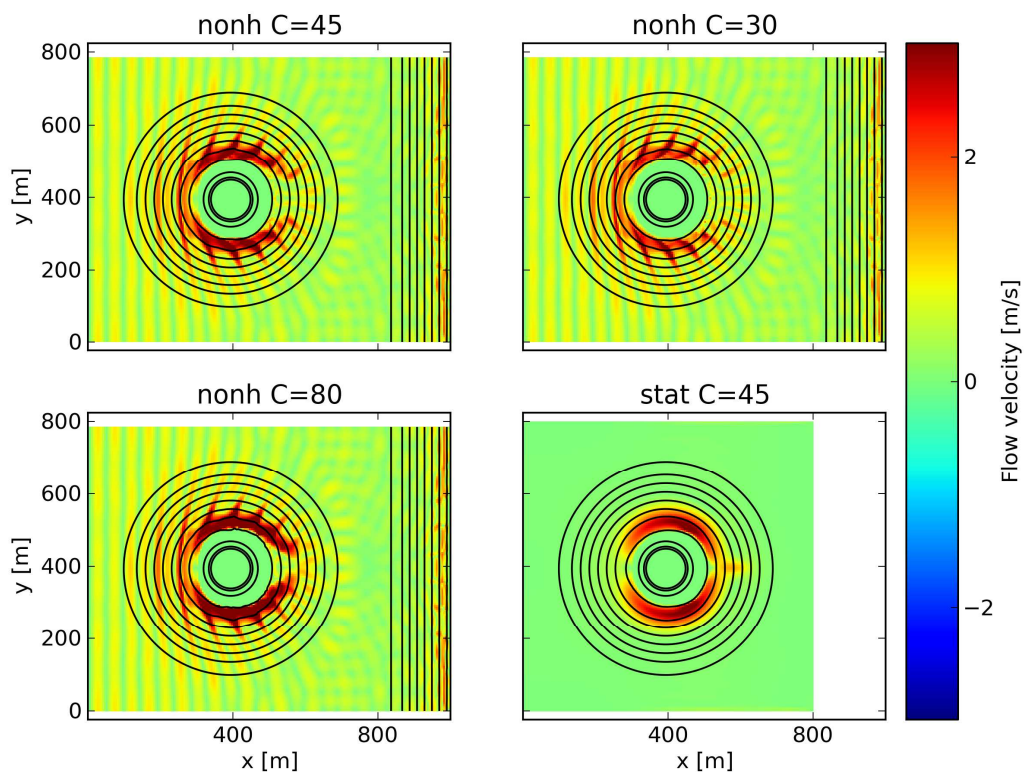


Figure 5 Magnitude of flow velocity (snapshot) in initial stage around a circular with different roughness for non-hydrostatic and stationary mode (bottom right); depth contours from + 8 to -12 m with 2 m intervals and -15 m.

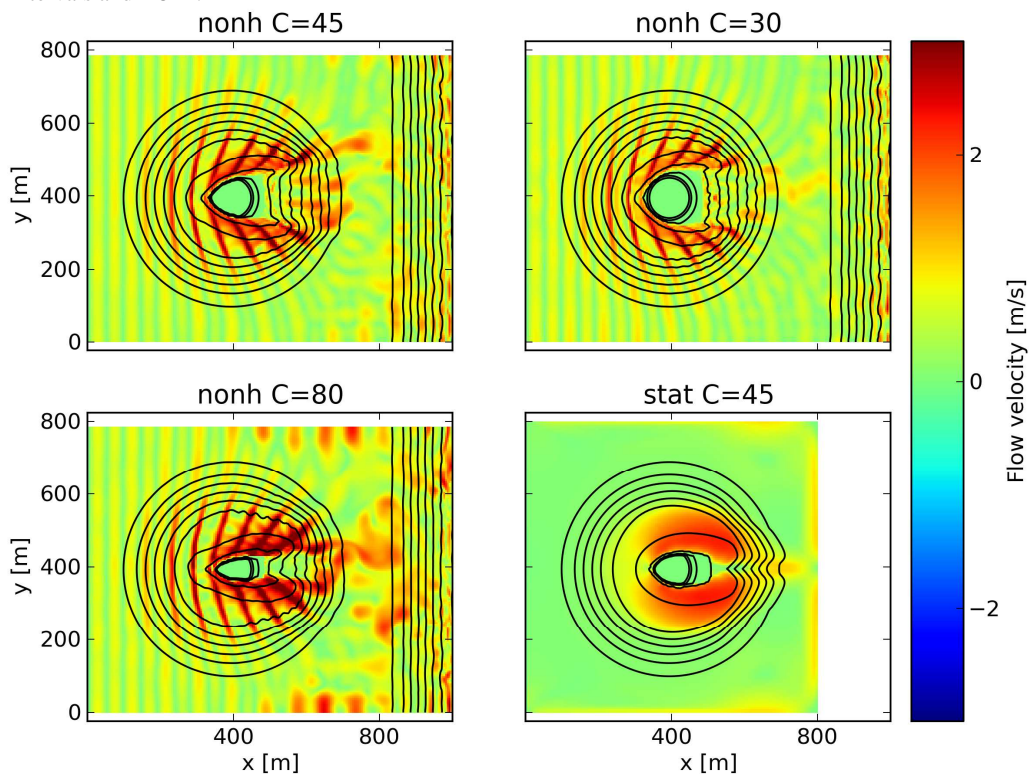


Figure 6 Magnitude of flow velocity (snapshot) after 10 hrs around a circular island, with different roughness for non-hydrostatic and stationary mode (bottom right); depth contours from + 8 to -12 m

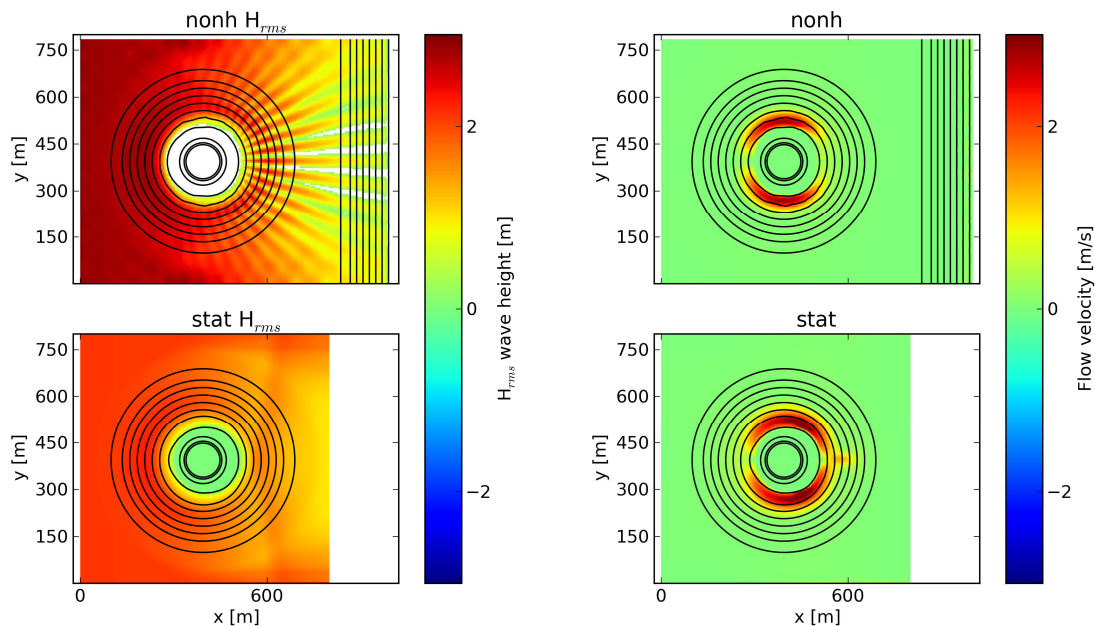


Figure 7 Mean wave height pattern for nonhydrostatic (top left) and stationary model (bottom left) and corresponding mean current patterns (right panels)

4. Morphodynamic evolution of a curved island coast

In order to investigate the processes involved in dune erosion along a curved coastline and the effect of the coastal radius, Den Heijer (2013) performed a series of XBeach simulations with arc shaped shorelines with different radii. In all models the cross-shore profile is alongshore uniform and the coastal arc is circular, ranging over 180 degrees. Five radii are investigated, ranging from 1900 m to 9500 m, which are one or two orders of magnitude larger than the Kamphuis islands from the previous section. The incident wave direction is shore normal in the middle of the arc. Figure 3 (top left) gives an impression of the bathymetry and the curvilinear grid. The bed level ranges from MSL-20 m at the offshore boundary to MSL+15 m at the dune crest. All simulations, five hours in duration use time invariant typical Dutch design storm conditions characterized by a storm surge water level of MSL+5 m, a significant wave height of 9 m and peak wave period of 12 s.

In all simulations, the erosion volume is primarily dependent on the location along the coastal arc, and less so on the coastal radius. Figure 8 (top right) shows the erosion volume in time along the coastline for the case with a radius of 1900 m. The maximum erosion occurs at the zones around 45 degrees with respect to the incident wave direction. Figure 8 (center left) shows the erosion volume along the coastline for different radii. The erosion pattern is similar for all radii, but the magnitude varies.

The results can be explained by the joint effect of alongshore varying wave setup, alongshore flow gradients and cross-shore flow pattern. At the middle of the arc, the wave setup is at its maximum and the alongshore current is zero. The alongshore current, as presented in Figure 8 (bottom right), increases towards its maximum at about 90 degrees. This maximum occurs typically at an angle larger than 45 degrees due to the refraction effects. The alongshore water level gradient is another driving force for the alongshore current. The cross-shore, offshore directed, velocities (Figure 8, bottom left) are almost constant in the region around normal wave incidence (between about -45 and 45 degrees) and fade out towards the lateral boundaries of the model. The absence of a clear peak in the cross-shore velocities at normal wave incidence can be explained by the 2D behavior. The demand for water to flow in alongshore direction

towards both lateral boundaries needs supply (onshore flow) at the location of normal wave incidence. This onshore flow obstructs the undertow and so prevents the clear peak in the cross-shore (offshore directed) flow velocities. This obstruction effect limits the cross-shore transport (Figure 8 center left) and is also the reason for the relatively limited erosion volumes at normal wave incidence. Intercomparison of simulations with different radii shows that the alongshore velocity is mainly dependent on the local incident wave angle w.r.t. the coast orientation rather than the radius.

As opposed to the small-scale islands in the previous section, which show strongly non-uniform alongshore behaviour, in the series of simulations discussed in this section the coastal radius is large with respect to the wave length. With increasing radius, more alongshore space is available for the refraction process. Since this larger scale curved coastlines do not cover the complete island, diffraction does not play a role here. Den Heijer (2013) shows that the erosion pattern as found for 9500 m radius is similar to a straight coast with varying incident wave angle. As a result, it can be stated that the larger radii in this series approach towards a quasi-alongshore uniform situation.

In conclusion, the dune erosion volume along a curved coastline is especially related to the wave angle relative to the local coastline orientation. This implies that the actual coastal radius is of minor importance

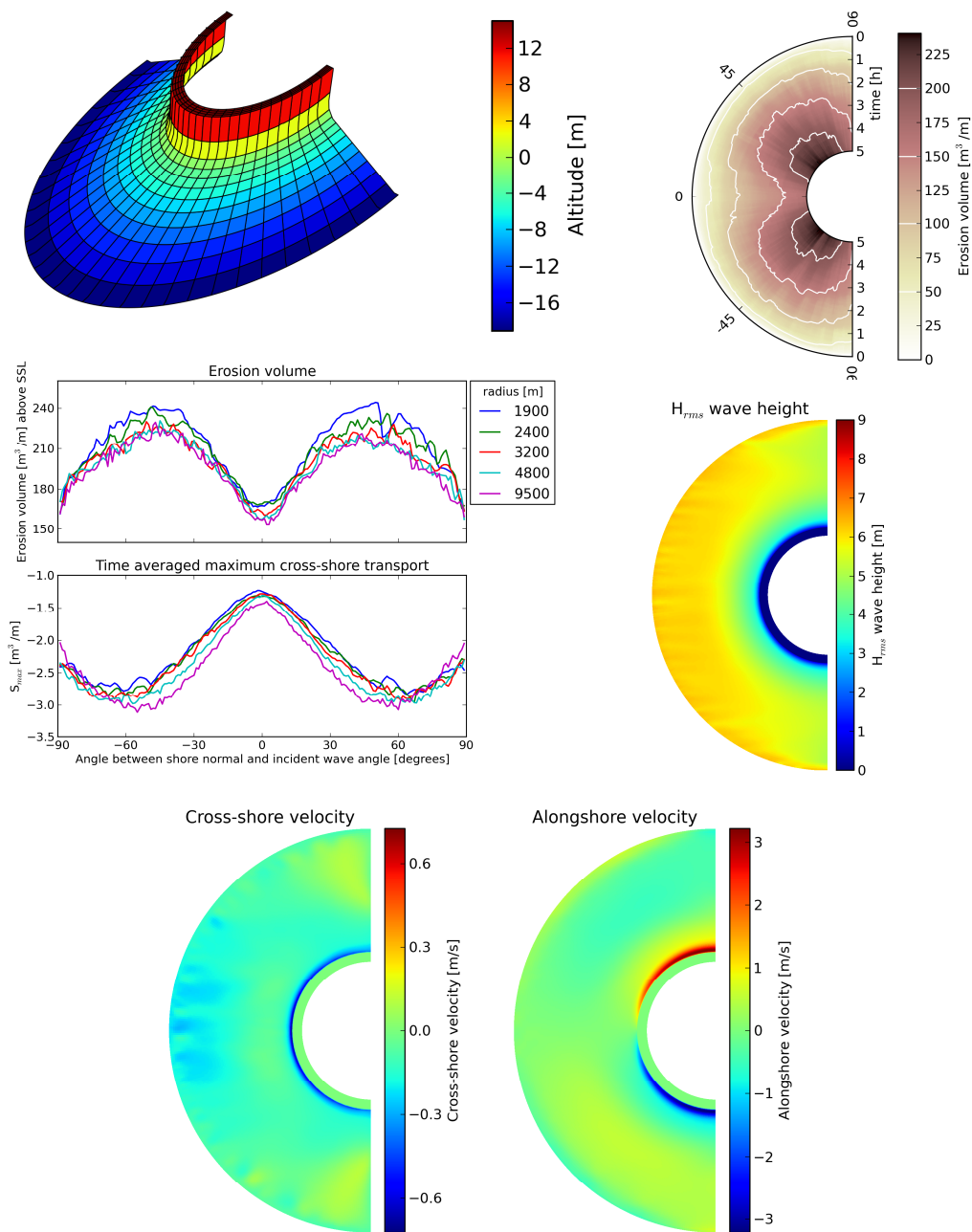


Figure 8 (top left) bathymetry and grid, erosion development in time (top right), erosion volume and cross-shore transport for various radii (center left), snapshot of wave height (center right), mean cross-shore current (bottom left) and mean alongshore current (bottom right)

5. Discussion

The cases as presented in this paper, involving strongly curved small-scale islands as well as larger scale curved coastlines, show the importance of representing both alongshore and cross-shore processes and their interactions. Therefore, classical coastline theory and other approaches that involve cross-shore processes only are not suitable for this type of problem. As a result of the curvature, large alongshore current

gradients are present and large alongshore flow velocities occur. Wave current interaction and sediment stirring due to alongshore current need to be properly represented to model this type of coastal curvature cases.

In both cases, described in this paper, a local erosion minimum is found at the upwind side of the island, where the incident wave direction is shore normal. When classifying dune erosion as a primarily cross-shore process, an erosion maximum would be expected at the islands' head. The modeling approach as applied in this paper shows that the maximum erosion is typically occurring at the location where cross-shore and alongshore processes optimally cooperate, being further downstream at about 45 degrees w.r.t. the main wave direction. At that location, the cross-shore processes (undertow) is still rather strong, while the relatively high (but not maximal) alongshore flow velocity facilitates the stirring of the sediment. At the head of the island, the alongshore flow velocity is zero, but alongshore flow in both directions is initiated. The supply needed, to fulfill the demand by the alongshore current flowing along both sides of the island, is for a large part coming from the offshore direction at the island head. This induces blocking of the undertow at that this location, and so obstructing the cross-shore erosion process.

The morphological behaviour of the nonhydrostatic model is quite promising, even though no changes at all were made to the sediment transport formulations; the main difference is that in the wave-averaged approach the mean current and orbital velocity are treated separately, whereas in the nonhydrostatic approach there is only one velocity, which fluctuates on all timescales. The model is capable of handling the runup and avalanching processes without problem and can erode the whole island away without numerical problems. It automatically produces skewness and asymmetry and related transports, as well as the depth-averaged return flow. All of these processes, however, need careful validation for which much more validation data from lab and field is needed.

Acknowledgements

Part of this research was funded by the Dutch Technology Foundation STW "The role of bathymetry, wave obliquity and coastal curvature in dune erosion prediction" (project 10196) and Deltares Strategic Funding in the framework of the "Event-driven hydro and morphodynamics" (project 1202362) program.

References

- Den Heijer, C. (2013). The role of bathymetry, wave obliquity and coastal curvature in dune erosion prediction. PhD thesis, Delft University of Technology. <http://dx.doi.org/10.4233/uuid:824df068-8046-414c-a1cc-7d159718918e>
- Kamphuis, J.W. and R.B. Nairn. (1984) Scale effects in large coastal mobile bed models. Proc. ICCE 1984.
- Pomeroy, A., R. Lowe, G. Symonds, A. van Dongeren and C. Moore (2012). The dynamics of infragravity wave transformation over a fringing reef. *J. Geophys. Res.*, 117, C11, doi:10.1029/2012JC008310.
- Roelvink, J.A., A. Reniers, A. Van Dongeren, J. Van Thiel de Vries, R. McCall, J. Lescinski. 2009. Modeling storm impacts on beaches, dunes and barrier islands. *Coastal Engineering*, doi: 10.1016/j.coastaleng.2009.08.006
- Roelvink, Dano, Stelling, Guus, Hoonhout, Bas, Risandi, Johan, Jacobs, Walter, Merli, Davide, (2012) Development and field validation of a 2dh curvilinear storm impact model, Proc. ICCE 2012, Santander.
- Smit, P.B., M. Zijlema and G.S. Stelling (2013), Depth-induced wave breaking in a non-hydrostatic, near-shore wave model. *Coastal Engineering* 76, doi:10.1016/j.coastaleng.2013.01.008.
- Stelling, G.S. and M. Zijlema (2003), An accurate and efficient finite-difference algorithm for non-hydrostatic free-surface flow with application to wave propagation. *International Journal For Numerical Methods In Fluids* 43, doi:10.1002/flid.595.
- Symonds, G., D. A. Huntley, and A. J. Bowen (1982), Two-dimensional surf beat: Long wave generation by a time-varying breakpoint, *J. Geophys. Res.*, 87(C1), 492–498, doi:10.1029/JC087iC01p00492.
- Zijlema, M. and G.S. Stelling (2005), Further experiences with computing non-hydrostatic free-surface flows involving water waves, *International Journal For Numerical Methods In Fluids* 48, doi:10.1002/flid.821.
- Zijlema, M. and G.S. Stelling (2008), Efficient computation of surf zone waves using the nonlinear shallow water equations with non-hydrostatic pressure. *Coastal Engineering* 55, doi:10.1016/j.coastaleng.2008.02.020.